

## Strongly Metastable Assemblies of Particles at Liquid Interfaces

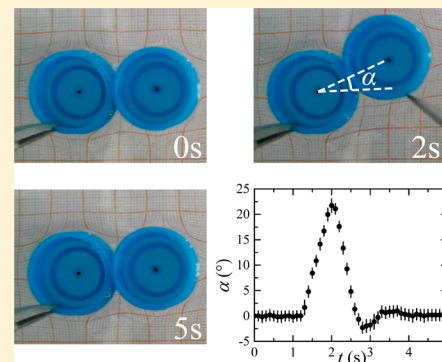
Nan Xue,<sup>†</sup> Shuai Wu,<sup>†,‡</sup> Sijie Sun,<sup>†</sup> David Quéré,<sup>\*,§</sup> and Quanshui Zheng<sup>\*,†,‡</sup>

<sup>†</sup>Department of Engineering Mechanics and <sup>‡</sup>Center for Nano and Micro Mechanics, Tsinghua University, Beijing 100084, China

<sup>§</sup>Physique et Mécanique des Milieux Hétérogènes, UMR 7636 du CNRS, ESPCI, 75005 Paris, France

### Supporting Information

**ABSTRACT:** The self-assembly of floating particles is a widely observed phenomenon. Ideally, rafts of identical floating spheres or cylinders should assemble in a closed-packed fashion. However, rafts are observed to exhibit large and various defects, and we show that the conjunction of lateral liquid bridges between particles and contact angle hysteresis freezes the rotation of particles around their neighbors, a mechanism that generates imperfect rafts. Conversely, we demonstrate how this capillary bond can be exploited to sculpt 2D aggregates far from equilibrium that are persistent.



### INTRODUCTION

Dense (or buoyant) particles at liquid surfaces interact owing to the deformation they generate at the surface. Nicolson<sup>1</sup> was the first to suggest that similar spheres floating at the surface of a pool tend to attract each other (Figure 1a). As shown by Kralchevsky et al.,<sup>2–4</sup> this so-called lateral flotation force (LFF) is quite general. The attraction takes place provided the floating bodies have similar menisci: as the particles are brought into contact, a fraction of these menisci are suppressed, which leads to a decrease in surface energy. This argument implies that the range of the interaction is the range of the menisci, that is, a few times the capillary length, typically around 1 cm. Vella<sup>5</sup> and Abkarian<sup>6</sup> pointed out that the resulting pair is heavier and slightly sinks so that the LFF may also have a gravitational component. However, similar interactions can still be observed on a much smaller scale where gravitational effects are negligible: if the particles are irregular (physically or chemically), then they also deform the interface on which they sit, which again generates an attraction, as studied more particularly by Loudet,<sup>7</sup> Yu,<sup>8</sup> Stebe,<sup>9,10</sup> and Vermant.<sup>11</sup>

These arguments allow us to understand that a triplet of floating particles similarly tends to adopt a compact shape once the two-body interactions have formed it, as sketched in Figure 1b. The surface energy of the triplet is a function of its internal angle  $\phi$ , and this energy can be evaluated using Surface Evolver<sup>12</sup> for the configuration of three cylinders of radius  $R$  floating on their base. If we calculate the surface area and plot the corresponding surface energy (normalized by the natural scale  $\gamma R^2$ , where  $\gamma$  is the liquid surface tension) as a function of  $\phi$  (Figure 1c), we observe that the looser the structure (that is, the larger  $\phi$ ), the larger the surface energy, which becomes a minimum for the most compact state ( $\phi = 60^\circ$ ): triplets should spontaneously close. More details on this simulation are given

in the Supporting Information, and similar calculations of surface energy in self-assembled particles can be found in refs 13 and 14.

In most cases, particles at interfaces are not restricted to pairs or triplets, and many particles form a raft, which can eventually sink if it is too large.<sup>6,7</sup> Again, we expect to reach the minimum in energy if the assembly is compact,<sup>14–16</sup> but rafts self-organizing from a random aggregation of particles are most often far from being dense,<sup>17–20</sup> which primarily arises from the jamming of subunits as they condense. We show in Figure 1d such a raft made of centimeter-sized polyethylene balls seen from the top as it reaches its final equilibrium state: obviously a metastable state as attested to by the presence of holes of various sizes inside the raft. But Figure 1d makes it clear that loose packing also arises from the presence of rigid subunits (three of them are stressed with circles) for which the balls would have enough space and time to reorganize but keep a noncompact shape, in contradiction to the attraction described in Figure 1b,c.

Our aim in this letter is to show that hydrophilic particles in contact indeed have rigid bonds, which prevents them from freely rotating. We interpret this rigidity as arising from the existence of lateral liquid bridges between the contacting particles, which, if contact angle hysteresis is present and the forces exerted on the particles not too large, have the ability to act as capillary springs between particles.

Received: October 3, 2014

Revised: November 17, 2014

Published: November 17, 2014



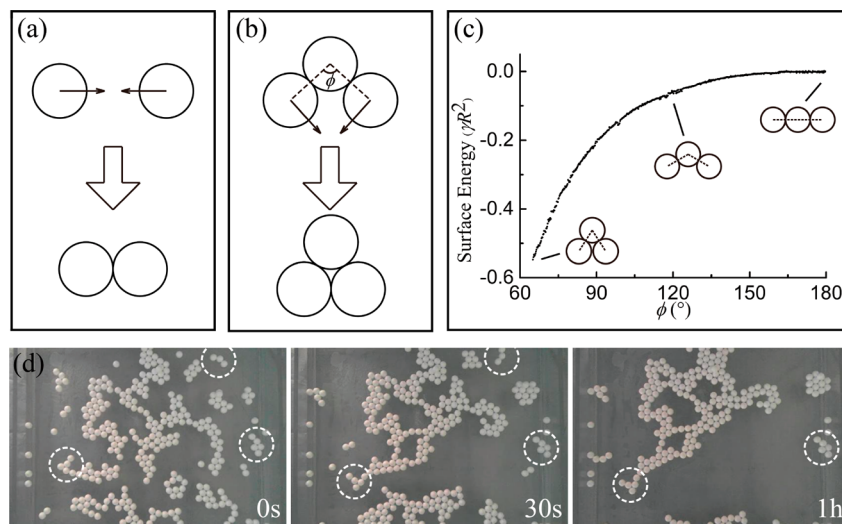


**Figure 1.** (a) Two particles floating at a liquid surface attract each other provided the floating bodies have similar menisci. (b) Similarly, a triplet of floating particles should tend to condense (close packing). (c) By calculating the surface energy of different configurations for the triplet (calculation done with Surface Evolver), it is indeed observed that the minimum in surface area (and hence surface energy) is reached for close packing. (d) Top view of an assembly of polyethylene spheres (diameter of 10 mm) at a water surface. If close enough, spheres aggregate, but many subunits (three of them are stressed by dotted circles) exhibit persistent open structures participating to the loose character of the draft. Images are taken at the end of the process of aggregation: a few events still happen between pictures 1 and 2 (separated by 30 s), but picture 3 (1 h later) shows that the evolution then becomes extremely slow.

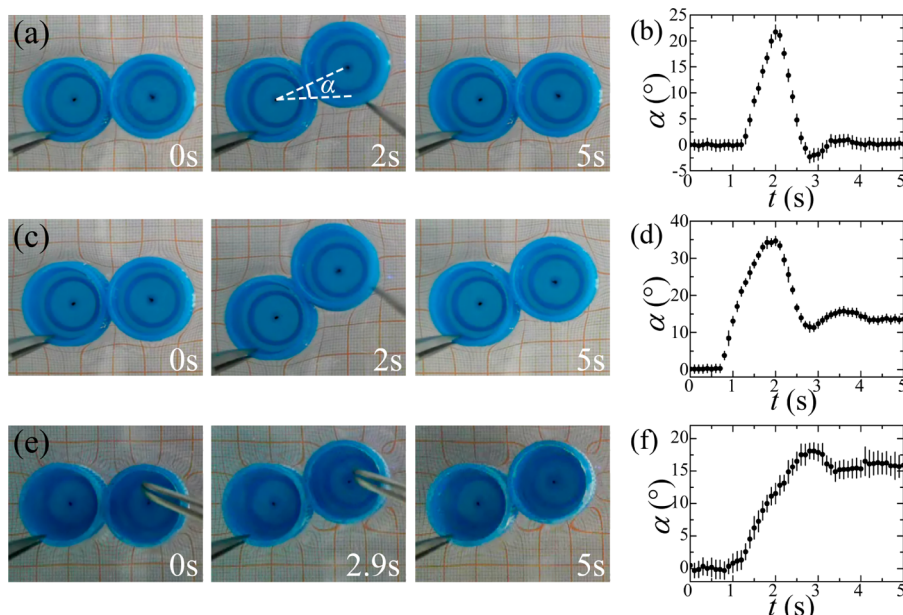


**Figure 2.** (a) Top view of a pair of floating caps and test of the rigidity of the bond between them. The left cap is kept fixed by a tweezers, and its neighbor brought into contact by capillary attraction is free. If we force its rotation by an angle  $\alpha$  (second photograph), then the angle relaxes to its initial value, showing the existence of a rigid bond between particles. (b) Time evolution of  $\alpha$  in the experiments. (c, d) Same experiment as in (a) and (b) but with the imposition of a rotation of the free cap of 35° instead of 21°. (e, f) The same caps treated hydrophobically also attract each other, but the behavior is observed to be very different: the angle remains at the imposed value (no relaxation), showing that the bond disappears when there is no bridge between the caps.

## EXPERIMENTAL METHODS

To test the ability of floating particles to rotate around each other (and thus to rearrange), we built a model experiment on a single bond, that is, on a single pair of particles. We consider centimeter-size cylinders (made of identical bottle caps of height  $H = 10$  mm, diameter  $2R = 20$  mm, and mass  $m = 1.1$  g) and place them on the surface of a large (metric) pool of water. A grid is placed below the transparent container of water, both to provide a scale (thin and thick lines delimit millimeter- and centimeter-sized cells, respectively) and to monitor the

deformation of the water surface from the distortion of the grid. The device and its evolution are followed from the top with a hang-up camera.

## RESULTS AND DISCUSSION

In this experiment, a first cap is fixed with tweezers, and the second one is left free: when placed about 1 cm from the first one, the free cap is first attracted by the fixed one, and the menisci responsible for flotation and attraction are visible in

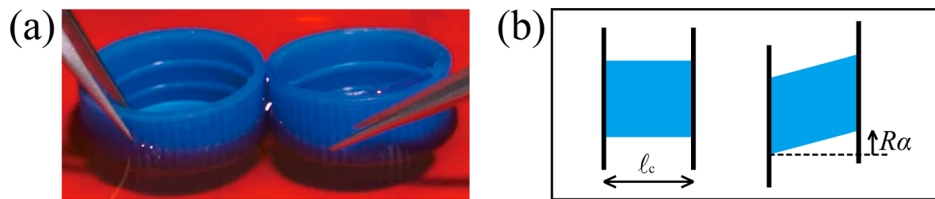


**Figure 3.** (a) Side view of a pair of floating caps of radius  $R$  (Movie 2 in Supporting Information). In a hydrophilic situation, a meniscus rises between the caps and binds them together. (b) General sketch (top view) of a bridge binding two solids. The bridge, of characteristic width  $l_c$  (the capillary length), is shown before and after a displacement of one solid by a distance  $R\alpha$  (corresponding to a rotation by a small angle  $\alpha$  for caps), assuming that the contact lines remain pinned.

Figure 2a. We define as a reference axis the line joining the caps' centers, and we force with another pair of tweezers the second cap to rotate by an angle  $\alpha$  from this axis (Figure 2a, second image). This angle is increased up to a maximum value of  $\alpha_M$  (here of about  $21^\circ$ , reached after 2 s); left free from this position, the cap is observed to recover its initial position of  $\alpha = 0$  in about 1 s (Figure 2a, third image). The whole process is filmed (Movie 1 in Supporting Information), and the variation of  $\alpha$  as a function of time  $t$  is plotted in Figure 2b. A rebound is observed as relaxation occurs, which shows that the dynamics of the process is dominated by inertia.

If close contact between caps is maintained, then all positions  $\alpha$  are equivalent in term of surface and gravitational energies. However, we observe in Figure 2a,b a memory effect: even if a significant rotation is applied, then the second cap is brought back to its initial position, which implies the existence of a springlike link between contacting caps. We interpret the existence of this rigid bond as arising from lateral liquid bridges.<sup>2–4</sup> We consider here the most common situation of a solid partially wet by water (hydrophilic situation, with a contact angle smaller than  $90^\circ$ ) so that liquid can rise in the confined region close to the contact, as seen in Figure 3a. If the resulting liquid bridge were ideal (with a unique contact angle given by the ideal Young relationship), then this bridge would reinforce the attraction between adjacent caps but would not generate a restoring force such as observed in Figure 2a,b. However, partial wetting is (nearly) always accompanied by contact angle hysteresis:<sup>21–23</sup> the bridge pins along the caps so that the rotation will deform only the lateral liquid interfaces (keeping the contact lines pinned, see Movie 2 in Supporting Information) if the prescribed angle  $\alpha$  is not too large. Hence, the conjunction of a liquid bridge with line pinning can generate a torque opposing the deformation of the bridge imposed by rotation. We measured contact angles of water on our caps and found advancing and receding angles with respective values of  $84 \pm 5$  and  $16 \pm 6^\circ$ , showing a large hysteresis of  $68^\circ$ . This large value arises from our choice of caps with splines and grooves all along the side: these textures provide strong pinning sites for the contact line, which generates a large hysteresis, a favorable situation for evidencing rigid bonds between adjacent particles.

As seen in Figure 3a, the lateral bridge lies along the whole height  $H$  of the caps (of radius  $R$ ). The bridge is simplified and sketched in Figure 3b, where top views show water menisci of height  $H$  and width  $l_c$  (the capillary length, which is about 2.5 mm for water), the typical width expected for menisci in corners. We assume that the contact line remains pinned as the right solid is displaced by a distance  $R\alpha$ , corresponding to a rotation by a small angle  $\alpha$  for caps. Only the liquid/vapor surface area varies as the bridge is sheared so that the increase in surface energy scales as  $\gamma HR^2\alpha^2/l_c$  for small displacements.

Hence we deduce a typical binding force varying as  $\gamma H R \alpha / l_c$ . This binding force is elastic: for a displacement  $\delta = R\alpha$ , it can be written as  $K\delta$ , where the stiffness  $K = \gamma H / l_c$  is scaled by the liquid surface tension  $\gamma$ . For angles on the order of  $20^\circ$ , the magnitude of this force is on the order of 1 mN, that is, large enough to resist perturbations on the surface of water, as observed experimentally. A more detailed derivation of the restoring torque with a two-cap system is given in the Supporting Information.

This general scenario has two natural consequences for the capillary bonds between caps: (i) If increasing the displacement, contact angles can reach either the receding angle or the advancing angle on the solid, which induces the motion of the line and thus the breakage of the link. Hence we expect a critical angle of rotation for the caps, above which the system cannot relax to its initial state. (ii) Lateral bridges such as observed in Figure 3a should not exist for hydrophobic caps, so that the binding force should vanish in this limit. We successively explore these two ideas.

We first show in Figure 2c,d an experiment similar to that in Figure 2a,b (Movie 1 in Supporting Information), where the second cap is now rotated around the first one by an angle  $\alpha_M = 35^\circ$  instead of  $21^\circ$ . As seen in the photographs and in the time evolution of  $\alpha$ , the angle also relaxes (final value  $\alpha_f = 13^\circ$ ), yet without recovering its initial state ( $\alpha = 0^\circ$ ). At such large deformations, the contact lines are forced to move along the lateral walls of the cap so that the initial position cannot be recovered. However, the bridge remains "loaded" in this case, which leads to a partial relaxation by about  $20^\circ$ .

We can suppress lateral bonds by working with hydrophobic caps. To keep the geometry unchanged, we worked with the same caps as previously, yet treated with a solution of Ultra Ever Dry (provided by Ultra Tech), which consists of hydrophobic colloids that stick to the surface, making it both hydrophobic and microrough and hence water-repellent. Measurements of advancing and receding contact angles of water on this modified surface are  $136 \pm 10$  and  $106 \pm 12^\circ$ , respectively, whose high values and reduced hysteresis confirm the efficiency of the treatment. With such angles, we expect no capillary rise between contacting caps and thus no bridge. Indeed, we see in Figure 2e,f (Movie 3 in Supporting Information) that despite the persistence of an attraction between the caps, the rotation of one relative to the other does not produce a memory effect anymore: if we plot the deformation as a function of time, then the final angle is found to remain very close to the imposed angle ( $\alpha_f \approx \alpha_M$ ) for a deformation of  $\alpha_M \approx 17^\circ$  for which a complete relaxation was observed with hydrophilic caps.

These different observations can be made more systematic by measuring the final observed angle  $\alpha_f$  as a function of the imposed angle  $\alpha_M$  (starting in all cases from  $\alpha = 0$ , as defined

above). The results for about 150 experiments done with 10 pairs of hydrophilic caps are displayed in Figure 4 (black circles) and compared to data obtained with hydrophobic caps (red squares). As for hydrophilic caps, three regions can be distinguished in this plot. (1) Below  $\alpha_c = 15\text{--}20^\circ$ , the final angle  $\alpha_f$  essentially is the initial one ( $\alpha_f \approx \alpha = 0$ ): the restoring force fully acts, and the bond between particles can be viewed as rigid. (2) Between  $15\text{--}20^\circ$  and  $60^\circ$ , the data become highly dispersed: we enter a region where the bond can be broken either because the rotation is not exactly performed in the same way or because pinning can differ between caps. For a bond arising from contact line pinning, the results should fluctuate as the contact angle hysteresis does when measured on different samples or at different locations for a given sample. In this region, the average final angle starts to increase with the applied

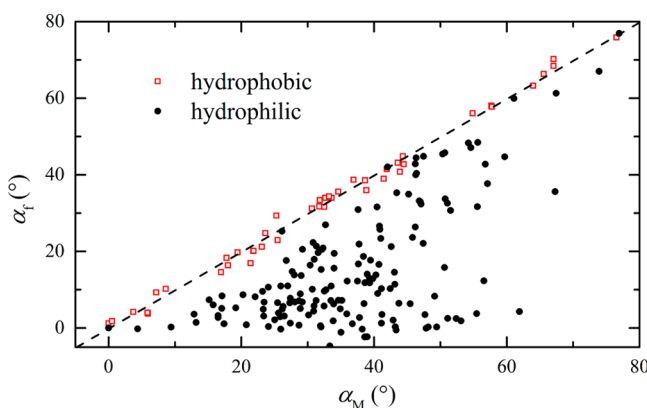


**Figure 4.** Final angle  $\alpha_f$  between two caps (defined relative to the axis between the caps' centers at their initial position) as a function of the angle  $\alpha_M$  imposed on one cap relative to the other (fixed) one for hydrophilic and hydrophobic caps (black circles and red squares, respectively). The equation  $\alpha_f = \alpha_M$  is drawn with a dotted line.

circles) and compared to data obtained with hydrophobic caps (red squares). As for hydrophilic caps, three regions can be distinguished in this plot. (1) Below  $\alpha_c = 15\text{--}20^\circ$ , the final angle  $\alpha_f$  essentially is the initial one ( $\alpha_f \approx \alpha = 0$ ): the restoring force fully acts, and the bond between particles can be viewed as rigid. (2) Between  $15\text{--}20^\circ$  and  $60^\circ$ , the data become highly dispersed: we enter a region where the bond can be broken either because the rotation is not exactly performed in the same way or because pinning can differ between caps. For a bond arising from contact line pinning, the results should fluctuate as the contact angle hysteresis does when measured on different samples or at different locations for a given sample. In this region, the average final angle starts to increase with the applied

rotation, which defines a fragile bond. (3) Above  $60^\circ$ , data approach the line  $\alpha_f = \alpha_M$ , which implies a complete breakage of the bond under large shear. This behavior is systematically observed with hydrophobic caps, for which data nicely follow the simple law  $\alpha_f = \alpha_M$  whatever  $\alpha_M$ . The critical angle becomes so small in this case that we could not measure it with our device ( $\alpha_c \approx 0$ ). More generally,  $\alpha_c$  is expected to quantify the ability of lateral bridges to resist shear, and it thus can be seen as a quantity likely to influence the compactness of rafts forming as floating particles gradually condense.

Rigid bonds (i.e., large  $\alpha_c$ ) can be exploited to design aggregates of a given shape, and we show in Figure 5 how a close-packed triplet (Figure 5a) can be irreversibly opened with an obtuse angle (Figure 5b) or even aligned (Figure 5c) without collapsing: such shapes, once formed, can be kept unchanged for days or even weeks on a water surface. Larger or wider objects can of course be sculpted using this principle, and Figure 5d,e shows two such examples, the first one being a variation on the possibility of making circles and the second one showing an example of a regular open pattern, which again are both stable on the scale of our experiments (a few days).

## OUTLOOK

We showed in this article that bonds resisting shear generally exist between contacted particles floating on the surface of a partially wetting liquid. The rigidity of these bonds was interpreted as arising from the pinning of liquid bridges along the particles' sides. The strength of the bonds compares to the attractive or repulsive capillary interaction between particles, so we expect them to influence the aggregation of various sizes of particles provided that the capillary force dominates in these systems. As often occurs, contact angle hysteresis brings about some ability to resist forces,<sup>21–23</sup> as seen, for example, when a drop sticks on an incline, provided these forces are not too large. Often considered to be a drawback,<sup>21–23</sup> contact angle hysteresis can be exploited here to shape the assemblies of

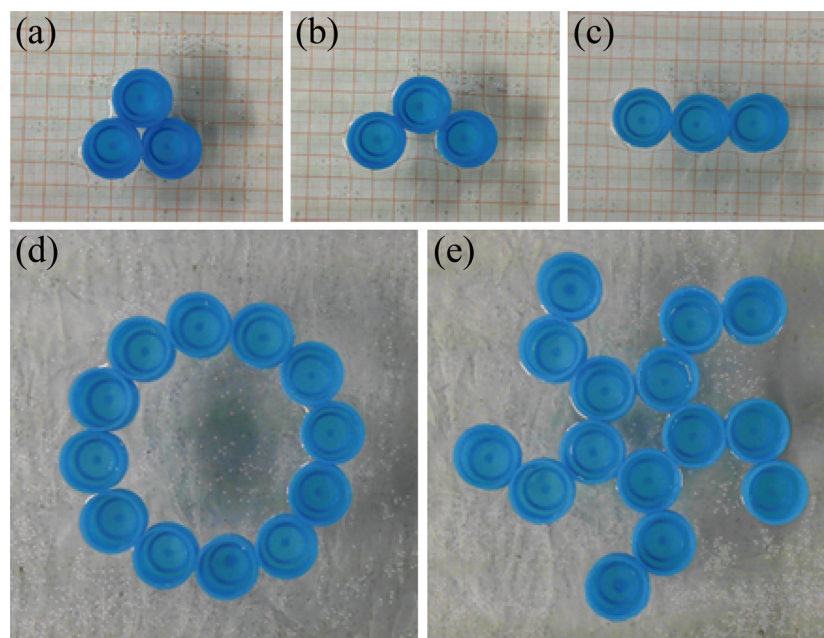


**Figure 5.** Existence of rigid bonds between hydrophilic particles can be exploited to sculpt aggregates. (a–c) Compact, open, and stretched triplets, respectively, that all persist for days, once made. (d) Circle of caps behaving as a rigid object: wind takes it without deforming it, and waves at the water surface do not modify its shape. (e) More compact structure with holes; there again, caps do not close-pack despite their proximity.

particles with a given design and a strong metastability, despite the existence of a compact state of smaller energy.

## ■ ASSOCIATED CONTENT

### S Supporting Information

Calculation details of Surface Evolver Programming. Derivation of scaling argument with two caps. Videos of caps operating by tweezers via top and side views. This material is available free of charge via the Internet at <http://pubs.acs.org>.

## ■ AUTHOR INFORMATION

### Corresponding Authors

\*E-mail: zhengqs@tsinghua.edu.cn.

\*E-mail: david.quere@espci.fr.

### Notes

The authors declare no competing financial interest.

## ■ ACKNOWLEDGMENTS

This work was financially supported by the NSFC under grant nos. 11072126 and 11272176, the Tsien Excellence in Engineering Program, and the Tsinghua Education Foundation. Suggestions from Wei Xiong, Yanshen Li, Jin Yang, and Cunjing Lv are acknowledged.

## ■ REFERENCES

- (1) Nicolson, M. M. The interaction between floating particles. *Proc. Cambridge Philos. Soc.* **1949**, *45*, 288–295.
- (2) Kralchevsky, P. A.; Nagayama, K. Capillary forces between colloidal particles. *Langmuir* **1994**, *10*, 23–36.
- (3) Kralchevsky, P. A.; Nagayama, K. Capillary interactions between particles bound to interfaces, liquid films and biomembranes. *Adv. Colloid Interface Sci.* **2000**, *85*, 145–192.
- (4) Kralchevsky, P. A.; Denkov, N. D. Capillary forces and structuring in layers of colloid particles. *Curr. Opin. Colloid Interface Sci.* **2001**, *6*, 383–401.
- (5) Vella, D.; Metcalfe, P. D.; Whittaker, R. J. Equilibrium conditions for the floating of multiple interfacial objects. *J. Fluid Mech.* **2006**, *549*, 215–224.
- (6) Abkarian, M.; Protière, S.; Aristoff, J. M.; Stone, H. A. Gravity-induced encapsulation of liquids by destabilization of granular rafts. *Nat. Commun.* **2013**, *4*, 1895.
- (7) Loudet, J. C.; Alsayed, A. M.; Zhang, J.; Yodh, A. G. Capillary interactions between anisotropic colloidal particles. *Phys. Rev. Lett.* **2005**, *94*, 018301.
- (8) Yu, Y.; Guo, M.; Li, X.; Zheng, Q. Meniscus-climbing behavior and its minimum free-energy mechanism. *Langmuir* **2007**, *23*, 10546–10550.
- (9) Lewandowski, E. P.; Cavallaro, M., Jr.; Botto, L.; Bernate, J. C.; Garbin, V.; Stebe, K. J. Orientation and self-assembly of cylindrical particles by anisotropic capillary interactions. *Langmuir* **2010**, *26*, 15142–15154.
- (10) Botto, L.; Yao, L.; Leheny, R. L.; Stebe, K. J. Capillary bond between rod-like particles and the micromechanics of particle-laden interfaces. *Soft Matter* **2012**, *8*, 4971–4979.
- (11) Madivala, B.; Fransaer, J.; Vermant, J. Self-assembly and rheology of ellipsoidal particles at interfaces. *Langmuir* **2009**, *25*, 2718–2728.
- (12) Brakke, K. A. The surface evolver. *Exp. Math.* **1992**, *1*, 141–165.
- (13) Fournier, J. B.; Galatola, P. Anisotropic capillary interactions and jamming of colloidal particles trapped at a liquid-fluid interface. *Phys. Rev. E* **2002**, *65*, 031601.
- (14) Schwenke, K.; Isa, L.; Del Gado, E. Assembly of nanoparticles at liquid interfaces: crowding and ordering. *Langmuir* **2014**, *30*, 3069–3074.
- (15) Aubry, N.; Singh, P.; Janjua, M.; Nudurupati, S. Micro-and nanoparticles self-assembly for virtually defect-free, adjustable monolayers. *Proc. Natl. Acad. Sci. U.S.A.* **2008**, *105*, 3711–3714.
- (16) Singh, P.; Joseph, D. D. Fluid dynamics of floating particles. *J. Fluid Mech.* **2005**, *530*, 31–80.
- (17) Vella, D.; Kim, H. Y.; Aussillous, P.; Mahadevan, L. Dynamics of surfactant-driven fracture of particle rafts. *Phys. Rev. Lett.* **2006**, *96*, 178301.
- (18) Benkoski, J. J.; Jones, R. L.; Douglas, J. F.; Karim, A. Photocurable oil/water interfaces as a universal platform for 2-D self-assembly. *Langmuir* **2007**, *23*, 3530–3537.
- (19) Berhanu, M.; Kudrolli, A. Heterogeneous structure of granular aggregates with capillary interactions. *Phys. Rev. Lett.* **2010**, *105*, 098002.
- (20) Garbin, V.; Crocker, J. C.; Stebe, K. J. Nanoparticles at fluid interfaces: Exploiting capping ligands to control adsorption, stability and dynamics. *J. Colloid Interface Sci.* **2012**, *387*, 1–11.
- (21) Johnson, R. E.; Dettre, R. H. Contact angle, wettability, and adhesion. *Adv. Chem. Ser.* **1964**, *43*, 112.
- (22) Joanny, J. F.; De Gennes, P. G. A model for contact angle hysteresis. *J. Chem. Phys.* **1984**, *81*, 552–562.
- (23) Quéré, D. Wetting and roughness. *Annu. Rev. Mater. Res.* **2008**, *38*, 71–99.